Modal Theory of Spatially Periodic Media

RUEY-SHI CHU, MEMBER, IEEE, AND JIN AU KONG, SENIOR MEMBER, IEEE

Abstract—**The modal theory is developed for a slab periodic medium bounded by different media on both sides. Dispersion analysis is carried out for the various cases. Wave amplitudes are determined from boundary conditions for electromagnetic field components. The results are compared and reduced to the well-known theories under simplified conditions. Analysis and calculations are aimed at applications to grating couplers, electrooptical modulators, and distributed feedback systems in integrated optics.**

I. Introduction

IN INTEGRATED OPTICS, a spatially periodic medium is useful in modeling many different situations, whether it be a grating coupler, a distributed feedback laser system, or an electrooptical modulator with periodically placed electrodes. A rigorous approach to the guided wave theory of light diffraction by a periodic slab medium was formulated and solved by Chu and Tamir [1]. They considered a plane wave incident at the Bragg angle upon a periodically modulated slab medium bounded on both sides by the same media. The direction of periodicity is assumed to be parallel to the boundary, and the effective modulation index of the periodic medium is assumed to be much smaller than unity.

Peng *et al.* [2] considered the problem of a slab periodic medium bounded by two different media. The direction of periodicity is also assumed to be parallel to the boundary surfaces. With applications to holography, Bernstein and Kermisch [3] treated a slab periodic medium bounded by the same media but with the direction of periodicity making an angle with respect to the boundary surfaces. The problem is also studied by Kogelnik [4] by using the coupled wave theory.

In this paper we study the problem of a plane wave incident, either normal or at the Bragg angle, upon a periodically modulated slab medium bounded by different media on its two sides. The direction of periodicity makes an angle with respect to the interfaces (Fig. 1). The solutions are expressed in terms of matrix formulation which can be readily calculated with a computer. We discuss dispersion characteristics by using load line concepts. Two special cases, with the axis of modulation parallel and perpendicular to the interfaces, are treated in detail. We then use the model to compute diffracted field components for a large range of effective modulation indices and to compare with other theories.

Manuscript received January 26, 1976; revised April 29, 1976. This work was supported by the Joint Services Electronics Program under Contract DAAB07-75-C-1346.

R. S. Chu is with the Communication Systems Division, GTE Sylvania, Inc., Needham, MA 02194.

J. A. Kong is with the Department of Electrical Engineering and Computer Science and the Research Laboratory of Electronics, Massachusetts Institute of Technology, Cambridge, MA 02139.

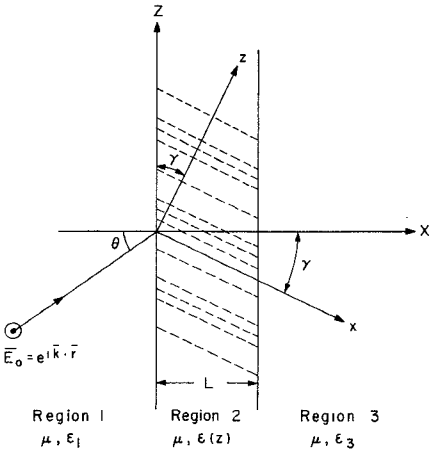

Fig. 1. Geometrical configuration.

II. Waves in Spatially Periodic Media

Consider a slab of spatially periodic medium of thickness L (Fig. 1). The direction of striation is along $\hat{x}$ and its axis of modulation is along $\hat{z}$. The boundaries of the slab are parallel to the Z axis at $X = 0$ and $X = L$, and their normals are parallel to $\hat{X}$. The angle between the z axis and the Z axis is γ. The relationships between the two systems of coordinates are

$$\left.\begin{aligned} x &= X\cos\gamma - Z\sin\gamma \\ z &= X\sin\gamma + Z\cos\gamma \end{aligned}\right\}. \tag{1}$$

The slab occupies the space $0 \le X \le L$ and possesses permittivity of the following form:

$$\varepsilon(z) = \varepsilon_2\varepsilon_0\left[1 - M\cos\left(\frac{2\pi}{d}z\right)\right] \tag{2}$$

where d is the periodicity of the modulation, M is the index of modulation, and ε_2 is the relative permittivity in the absence of the modulation ($M = 0$). For $X \le 0$ the medium has a relative permittivity of ε_1 and for $X \ge L$ the medium has a relative permittivity of ε_3.

Inside the periodic medium we use the coordinates (x,y,z) and write the wave equation as

$$[\nabla^2 + \omega^2\mu_0\varepsilon(z)]\tilde{E}_{2y} = 0. \tag{3}$$

A modal solution to (3) can be written as

$$\tilde{E}_{2y}^{(\nu)}(x,z) = e^{i\tilde{\xi}_\nu x}\tilde{\phi}_\nu(z). \tag{4}$$

The mode function $\tilde{\phi}(z)$ satisfies the Mathieu differential equation.

$$\frac{d^2\tilde{\phi}_\nu(z)}{dz^2} + (\pi/d)^2\left(p_\nu - 2q\cos\frac{2\pi}{d}z\right)\tilde{\phi}_\nu(z) = 0 \tag{5}$$

with $k_0 = \omega/c = 2\pi/\lambda$,

$$pv = (d/\pi)^2(\varepsilon_2 k_0^2 - \tilde{\xi}_v^2) \tag{6}$$

$$q = 2(d/\lambda)^2 M\varepsilon_2. \tag{7}$$

The mode function $\tilde{\phi}_v(z)$ can be written as

$$\tilde{\phi}_v(z) = \sum_n a_{n-v}^{(v)} e^{i\tilde{\beta}_n^{(v)} z} \tag{8}$$

with

$$\tilde{\beta}_n^{(v)} = \tilde{\beta}_0^{(v)} + n\frac{2\pi}{d}, \qquad n = 0, \pm 1, \pm 2, \cdots. \tag{9}$$

The index v represents the particular mode v. Substitution of (8) in (5) yields

$$\left[\left(\frac{\tilde{\beta}_n^{(v)} d}{\pi}\right)^2 - p_v\right] a_{n-v}^{(v)} + q[a_{n-v-1}^{(v)} + a_{n-v+1}^{(v)}] = 0 \tag{10}$$

which can be written in the form of two continued fraction relations

$$\frac{a_r^{(v)}}{a_{r-1}^{(v)}} = -\frac{q}{L_r^v} \Big| - \frac{q^2}{L_{r+1}^v} \Big| - \frac{q^2}{L_{r+2}^v} \Big| - \cdots \tag{11}$$

$$\frac{a_{r-1}^{(v)}}{a_r^{(v)}} = -\frac{q}{L_{r-1}^v} \Big| - \frac{q^2}{L_{r-2}^v} \Big| - \frac{q^2}{L_{r-3}^v} \Big| - \cdots \tag{12}$$

with $r = n - v$ and

$$L_r^v = \left(\frac{\tilde{\beta}_v^{(v)} d}{\pi} + 2r\right)^2 - p_v, \qquad v, r = 0, \pm 1, \pm 2, \cdots. \tag{13}$$

The x-component wave numbers $\tilde{\xi}_v$ are found from p_v while p_v is determined by inverting either (11) or (12) and equating the result with the other. We obtain, for $r = 0$,

$$L_0^v = \left(\frac{q^2}{L_1^v} \Big| - \frac{q^2}{L_2^v} \Big| - \frac{q^2}{L_3^v} \Big| - \cdots\right) + \left(\frac{q^2}{L_{-1}^v} \Big| - \frac{q^2}{L_{-2}^v} \Big| - \frac{q^2}{L_{-3}^v} \Big| - \cdots\right). \tag{14}$$

This represents a transcendental relationship among the quantities q, p_v, and $\tilde{\beta}_0^{(v)}$. By substituting (6) and (7) into (14), we establish the dispersion relation for quantities k_0, $\tilde{\xi}_v$, and $\tilde{\beta}_0^{(v)}$.

As the modulation index M becomes zero, $L_0^v = 0$ and (6) and (13) yield

$$(\tilde{\xi}_v d/\pi)^2 + \left(\frac{\tilde{\beta}_0^{(v)} d}{\pi} + 2v\right)^2 = \varepsilon_2 (k_0 d/\pi)^2, \qquad v = 0, \pm 1, \pm 2, \cdots. \tag{15}$$

Equation (15) represents a set of circles centered at $\tilde{\beta}_0^{(v)} d/\pi = 0, \pm 2, \pm 4, \cdots$ with equal radius $\sqrt{\varepsilon_2}\,(k_0 d/\pi)$. When M is not zero but small, the dispersion curves do not deviate very much from the case when $M \to 0$ except near the intersection points of any of the two circles. At these intersection regimes the dispersion curves of the finite M case connect together without intersecting and produce stopbands where waves in the z direction become evanescent [5].

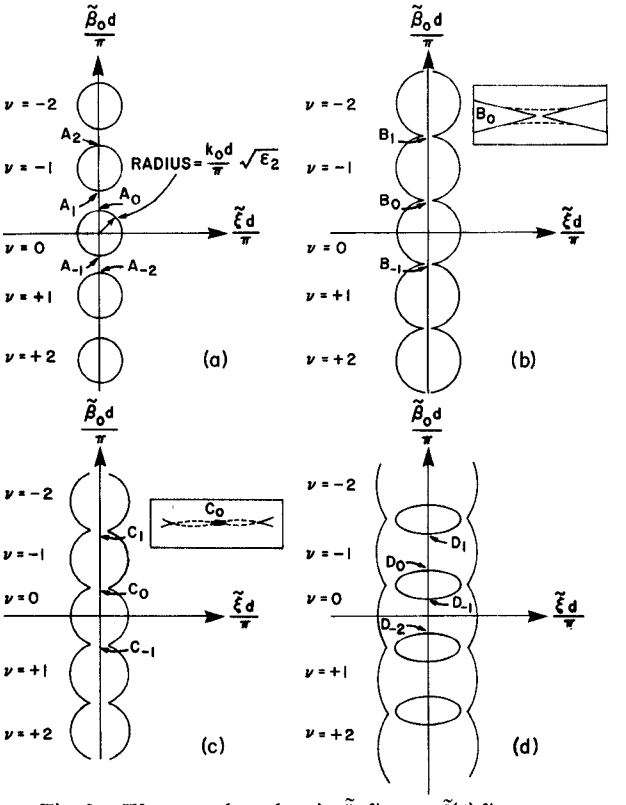

Fig. 2. Wave number plots in $\tilde{\xi}_v d/\pi$ and $\tilde{\beta}^{(v)} d/\pi$ space.

Consider the construction of the Brillouin $k_0 - \tilde{\beta}$ diagram from the wave number plots in $\tilde{\xi}_v d/\pi$ and $\tilde{\beta}_0^{(v)} d/\pi$ space for $\tilde{\xi}_v = 0$, i.e., waves propagate in the z direction. When k_0 is small such that $\sqrt{\varepsilon_2}\, k_0 d/\pi < 1$, the $\tilde{\beta}_0 d/\pi$ axis intersects the dispersion curves at $A_0, A_1, \cdots$, which are shown in Figs. 2(a) and 3. For $\sqrt{\varepsilon_2}\, k_0 d/\pi \approx 1$, the first stopband as shown in Fig. 3 is constructed from Fig. 2(b) and (c). As $1 < \sqrt{\varepsilon_2}\, k_0 d/\pi < 2$, we move into another passband in the Brillouin diagram as seen from Fig. 2(d) and Fig. 3. Note that

$$\tilde{\beta}_0^{(v)} = \tilde{\beta}_{-v}^{(0)} = \tilde{\beta}_0^{(0)} - v\frac{2\pi}{d} \tag{16}$$

and

$$\tilde{\beta}_n^{(v)} = \tilde{\beta}_0^{(0)} + (n - v)\frac{2\pi}{d} = \tilde{\beta}_{n-v}^{(0)}. \tag{17}$$

Thus the zeroth wave number $\tilde{\beta}_0^{(v)}$ of the vth mode is identical to the $-v$th wave number $\tilde{\beta}_{-v}^{(0)}$ of the zeroth mode. As a result, all the v modes are identical.

We now estimate the bandwidth of the stopband for the case of $q \ll 1$. From (6) and (7) we find

$$p = \varepsilon_2 (k_0 d/\pi)^2 = 2q/M. \tag{18}$$

It was shown that when $\tilde{\beta}_0^{(0)} d/\pi = 1$ and $q \ll 1$ we have

$$p \approx 1 \pm q. \tag{19}$$

The plus sign corresponds to the upper branch and the minus sign corresponds to the lower branch. Thus we have, for the upper branch,

$$\sqrt{\varepsilon_2}\,(k_0 d/\pi)_{UB} = [1 - (M/2)]^{-1/2}$$

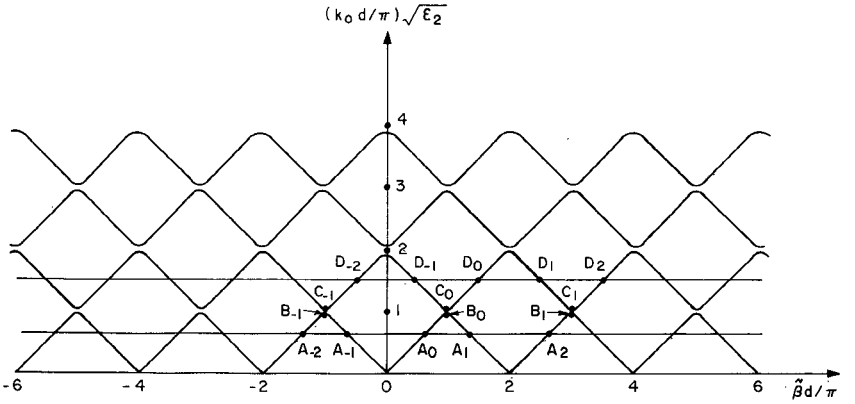

Fig. 3. Brillouin diagram constructed from Fig. 2.

and for the lower branch,

$$\sqrt{\varepsilon_2}\,(k_0 d/\pi)_{\mathrm{LB}} = [1 + (M/2)]^{-1/2}.$$

Forming the difference of the two equations, we find

$$\Delta = \sqrt{\varepsilon_2}\,(k_0 d/\pi)_{\mathrm{UB}} - \sqrt{\varepsilon_2}\,(k_0 d/\pi)_{\mathrm{LB}} \approx M/2.$$

Thus the bandwidth of the first stopband is proportional to the modulation index M.

III. Wave Amplitudes

A plane wave with the electric field in the $\hat{y}$ direction (TE wave) is incident upon the slab at an angle θ_0 with respect to the normal to the slab boundaries, i.e., the X axis. The solution in region 1 can be written as

$$E_{1y}(X,Z) = e^{ik_X X + ik_Z Z} + \sum_n R_n e^{-ik_{Xn}X + ik_{Zn}Z} \tag{20}$$

$$H_{1Z}(X,Z) = \frac{k_X}{\omega\mu} e^{ik_X X + ik_Z Z} - \sum_n \frac{k_{Xn}}{\omega\mu} R_n e^{-ik_{Xn}X + ik_{Zn}Z} \tag{21}$$

where

$$k_Z = k \sin\theta_0 = \sqrt{\varepsilon_1}\, k_0 \sin\theta_0 \tag{22}$$

$$k_X = k \cos\theta_0 = \sqrt{\varepsilon_1}\, k_0 \cos\theta_0 \tag{23}$$

$$k_{Zn} = k_Z + n\frac{2\pi}{d}\cos\gamma \tag{24}$$

$$k_{Xn} = (k^2 - k_{Zn}^2)^{1/2} = (\varepsilon_1 k_0^2 - k_{Zn}^2)^{1/2} \tag{25}$$

$n = 0, \pm 1, \pm 2, \cdots$, and $k_0 = 2\pi/\lambda = \omega/c$. Note that the periodicity at the boundaries is d sec γ rather than d. In region 3 ($X \geq L$), the transmitted wave takes the form

$$E_{3y}(X,Z) = \sum_n T_n e^{ik_{3Xn}(X-L) + ik_{Zn}Z} \tag{26}$$

where

$$k_{3Xn} = \left(\frac{\varepsilon_3}{\varepsilon_1}k^2 - k_{Zn}^2\right)^{1/2} = (\varepsilon_3 k_0^2 - k_{Zn}^2)^{1/2}. \tag{27}$$

In order to match boundary conditions at $X = 0$ and $X = L$, we substitute (8) in (4) and use the transformation (1) to get

$$E_{2y}^{(\nu)}(X,Z) = e^{i\tilde{\xi}_\nu(X\cos\gamma - Z\sin\gamma)} \sum_n a_{n-\nu}^{(\nu)} \cdot e^{i\tilde{\beta}_n^{(\nu)}(X\sin\gamma + Z\cos\gamma)}$$

$$= \sum_n a_{n-\nu}^{(\nu)} \cdot e^{i[(\tilde{\xi}_\nu\cos\gamma + \tilde{\beta}_n^{(\nu)}\sin\gamma)X + (-\tilde{\xi}_\nu\sin\gamma + \tilde{\beta}_n^{(\nu)}\cos\gamma)Z]}. \tag{28}$$

At the boundaries phase matching along Z yields

$$k_{Zn} = -\tilde{\xi}_\nu \sin\gamma + \tilde{\beta}_n^{(\nu)}\cos\gamma. \tag{29}$$

Introducing (24) and (9) into (29), we have

$$\tilde{\beta}_0^{(\nu)} = \tilde{\xi}_\nu \tan\gamma + k_Z \sec\gamma. \tag{30}$$

Equation (30) provides a linear relation between the two wave numbers $\tilde{\xi}_\nu$ and $\tilde{\beta}_0^{(\nu)}$ in modulated medium. The dispersion relation (14) provides another relation between the two quantities $\tilde{\xi}_\nu$ and $\tilde{\beta}_0^{(\nu)}$. Thus if we solve (14) and (30) simultaneously for $\tilde{\xi}_\nu$ and $\tilde{\beta}_0^{(\nu)}$, we obtain the entire set of characteristic wave numbers $(\tilde{\xi}_\nu, \tilde{\beta}_0^{(\nu)})$. This is illustrated graphically in Fig. 4. The line SS' represents (30) which intersects the dispersion curves at A, B, etc. The points A, B, and C refer to modes that are guided along the positive X direction, and the points A', B', and C' refer to modes that are guided along the negative X direction. We denote the set of eigenvalues that is guided along the positive X direction by $(\tilde{\xi}_{\nu+}, \tilde{\beta}_{0+}^{(\nu)})$ and the set of eigenvalues that is guided along the negative X direction by $(\tilde{\xi}_{\nu-}, \tilde{\beta}_{0-}^{(\nu)})$. Thus the fields in region 2 may be written as summations over the modes in the form

$$\tilde{E}_{2y}(X,Z) = \sum_\nu \left\{ \tilde{U}_\nu \sum_n a_{n-\nu}^{(\nu)} e^{i[(\tilde{\xi}_{\nu+}\cos\gamma + \tilde{\beta}_{n+}^{(\nu)}\sin\gamma)X + k_{Zn}Z]} + \tilde{V}_\nu \sum_n \bar{a}_{n-\nu}^{(\nu)} e^{i[(\tilde{\xi}_{\nu-}\cos\gamma + \tilde{\beta}_{n-}^{(\nu)}\sin\gamma)X + k_{Zn}Z]} \right\} \tag{31}$$

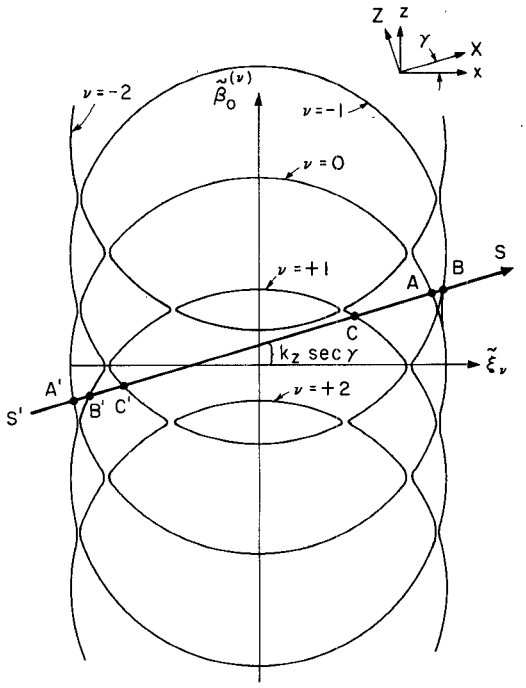

Fig. 4. Characteristic wave numbers determined with the load line SS'.

$$\tilde{H}_{2Z}(X,Z) = \sum_\nu \left\{ \tilde{U}_\nu \sum_n a_{n-\nu}^{(\nu)} \left(\frac{\tilde{\xi}_{\nu+} \cos\gamma + \tilde{\beta}_{n+}{}^{(\nu)} \sin\gamma}{\omega\mu} \right) \cdot e^{i[(\tilde{\xi}_{\nu+}\cos\gamma + \tilde{\beta}_{n+}{}^{(\nu)}\sin\gamma)X + k_{Zn}Z]} + \tilde{V}_\nu \sum_n \bar{a}_{n-\nu}^{(\nu)} \left(\frac{\tilde{\xi}_{\nu-}\cos\gamma + \tilde{\beta}_{n-}{}^{(\nu)}\sin\gamma}{\omega\mu} \right) \cdot e^{i[(\tilde{\xi}_{\nu-}\cos\gamma + \tilde{\beta}_{n-}{}^{(\nu)}\sin\gamma)X + k_{Zn}Z]} \right\} \quad (32)$$

where $a_{n-\nu}^{(\nu)}$ and $\bar{a}_{n-\nu}^{(\nu)}$ are determined from (11) and (12) for a given $(\tilde{\xi}_{\nu+}, \tilde{\beta}_{0+}{}^{(\nu)})$ and $(\tilde{\xi}_{\nu-}, \tilde{\beta}_{0-}{}^{(\nu)})$, respectively. The modal coefficients R_n, T_n, $\tilde{U}_\nu$, and $\tilde{V}_\nu$ are determined by matching boundary conditions at $X = 0$ and $X = L$.

At $X = 0$, the continuity of tangential $\bar{E}$ and $\bar{H}$ yields

$$\delta_{n0} + R_n = \sum_\nu (\tilde{U}_\nu a_{n-\nu}^{(\nu)} + \tilde{V}_\nu \bar{a}_{n-\nu}^{(\nu)}) \quad (33)$$

$$k_{Xn}(\delta_{n0} - R_n) = \sum_\nu [\tilde{U}_\nu a_{n-\nu}^{(\nu)}(\tilde{\xi}_{\nu+}\cos\gamma + \tilde{\beta}_{n+}{}^{(\nu)}\sin\gamma) + \tilde{V}_\nu \bar{a}_{n-\nu}^{(\nu)}(\tilde{\xi}_{\nu-}\cos\gamma + \tilde{\beta}_{n-}{}^{(\nu)}\sin\gamma)]. \quad (34)$$

At $X = L$, the continuity of tangential $\bar{E}$ and $\bar{H}$ yields

$$T_n = \sum_\nu [\tilde{U}_\nu a_{n-\nu}^{(\nu)} e^{i(\tilde{\xi}_{\nu+}\cos\gamma + \tilde{\beta}_{n+}{}^{(\nu)}\sin\gamma)L} + \tilde{V}_\nu \bar{a}_{n-\nu}^{(\nu)} e^{i(\tilde{\xi}_{\nu-}\cos\gamma + \tilde{\beta}_{n-}{}^{(\nu)}\sin\gamma)L}] \quad (35)$$

$$k_{3Xn}T_n = \sum_\nu [\tilde{U}_\nu a_{n-\nu}^{(\nu)}(\tilde{\xi}_{\nu+}\cos\gamma + \tilde{\beta}_{n+}{}^{(\nu)}\sin\gamma) \cdot e^{i(\tilde{\xi}_{\nu+}\cos\gamma + \tilde{\beta}_{n+}{}^{(\nu)}\sin\gamma)L} + \tilde{V}_\nu \bar{a}_{n-\nu}{}^{(\nu)}(\tilde{\xi}_{\nu-}\cos\gamma + \tilde{\beta}_{n-}{}^{(\nu)}\sin\gamma) \cdot e^{i(\tilde{\xi}_{\nu-}\cos\gamma + \tilde{\beta}_{n-}{}^{(\nu)}\sin\gamma)L}]. \quad (36)$$

Equations (33)–(36) can be cast in matrix form and solved by proper truncation to yield numerical answers. In the following two sections we consider the special cases of modulation axis parallel and perpendicular to the boundary surfaces of the slab.

IV. Axis of Modulation Parallel to Slab Interfaces

As a special case of the preceding general formulation, we consider the situation when $\gamma = 0$. We have

$$\tilde{\xi}_{\nu-} = \tilde{\xi}_{\nu+} = \tilde{\xi}_\nu \quad (37)$$

$$\tilde{\beta}_{n-}{}^{(\nu)} = \tilde{\beta}_{n+}{}^{(\nu)} = \tilde{\beta}_n^{(\nu)} = k_{Zn} = k_Z + n\frac{2\pi}{d}, \quad n = 0, \pm1, \pm2, \cdots \quad (38)$$

and $\bar{a}_{n-\nu}^{(\nu)} = a_{n-\nu}^{(\nu)}$.

The fields in the modulated region now reduce to

$$E_{2y}(X,Z) = \sum_\nu (\tilde{U}_\nu e^{i\tilde{\xi}_\nu X} + \tilde{V}_\nu e^{-i\tilde{\xi}_\nu X}) \sum_n a_{n-\nu}^{(\nu)} e^{i\tilde{\beta}_n{}^{(\nu)}Z} \quad (39)$$

$$H_{2Z}(X,Z) = \sum_\nu \frac{\tilde{\xi}_\nu}{\omega\mu} (\tilde{U}_\nu e^{i\tilde{\xi}_\nu X} - \tilde{V}_\nu e^{-i\tilde{\xi}_\nu X}) \sum_n a_{n-\nu}^{(\nu)} e^{i\tilde{\beta}_n{}^{(\nu)}Z}. \quad (40)$$

Equations (33)–(36) become

$$\delta_{n0} + R_n = \sum_\nu (\tilde{U}_\nu + \tilde{V}_\nu) a_{n-\nu}^{(\nu)} \quad (41)$$

$$k_{Xn}(\delta_{n0} - R_n) = \sum_\nu \tilde{\xi}_\nu (\tilde{U}_\nu - \tilde{V}_\nu) a_{n-\nu}^{(\nu)} \quad (42)$$

$$T_n = \sum_\nu (\tilde{U}_\nu e^{i\tilde{\xi}_\nu L} + \tilde{V}_\nu e^{-i\tilde{\xi}_\nu L}) a_{n-\nu}^{(\nu)} \quad (43)$$

$$k_{3xn}T_n = \sum_\nu \tilde{\xi}_\nu (\tilde{U}_\nu e^{i\tilde{\xi}_\nu L} - \tilde{V}_\nu e^{-i\tilde{\xi}_\nu L}) a_{n-\nu}^{(\nu)}. \quad (44)$$

Eliminating $\tilde{U}_\nu$ and $\tilde{V}_\nu$ from (41)–(44), we have

$$\begin{pmatrix} A & B \\ C & D \end{pmatrix} \begin{pmatrix} \boldsymbol{R} \\ \boldsymbol{T} \end{pmatrix} = \begin{pmatrix} \tilde{\boldsymbol{f}} \\ \tilde{\boldsymbol{g}} \end{pmatrix} \quad (45)$$

where

$$A = (a_{\nu n}) \qquad a_{\nu n} = a_{n-\nu}^{(\nu)} \left(\frac{k_{xn}}{\tilde{\xi}_\nu} - 1 \right) \quad (46)$$

$$B = (b_{\nu n}) \qquad b_{\nu n} = a_{n-\nu}^{(\nu)} \left(\frac{k_{3xn}}{\tilde{\xi}_\nu} + 1 \right) e^{-i\tilde{\xi}_\nu L} \quad (47)$$

$$C = (c_{\nu n}) \qquad c_{\nu n} = a_{n-\nu}^{(\nu)} \left(\frac{k_{xn}}{\tilde{\xi}_\nu} + 1 \right) \quad (48)$$

$$D = (d_{\nu n}) \qquad d_{\nu n} = a_{n-\nu}^{(\nu)} \left(\frac{k_{3xn}}{\tilde{\xi}_\nu} - 1 \right) e^{i\tilde{\xi}_\nu L} \quad (49)$$

$$\tilde{\boldsymbol{f}} = (\tilde{f}_\nu) \qquad \tilde{f}_\nu = a_{-\nu}^{(\nu)} \left(\frac{k_x}{\tilde{\xi}_\nu} + 1 \right) \quad (50)$$

$$\tilde{\boldsymbol{g}} = (\tilde{g}_\nu) \qquad \tilde{g}_\nu = a_{-\nu}^{(\nu)} \left(\frac{k_x}{\tilde{\xi}_\nu} - 1 \right) \quad (51)$$

and

$$\boldsymbol{R} = (R_n) \qquad \boldsymbol{T} = (T_n).$$

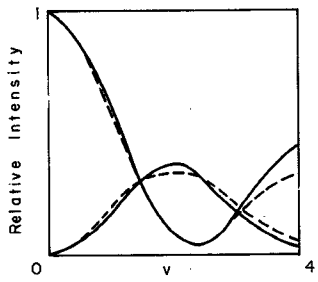

Fig. 5. The zeroth-order and the first-order transmitted relative intensities at normal incidence plotted as a function of v for $Q = 2$ and compared with results by Klein and Cook (dashed lines).

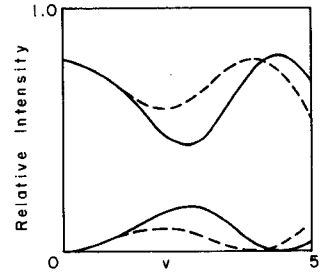

Fig. 6. The zeroth-order and the first-order transmitted relative intensities at normal incidence plotted as a function of v for $Q = 7$ and compared with results by Klein and Cook (dashed lines).

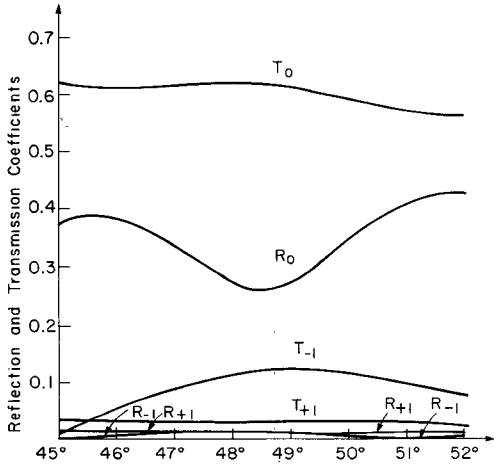

Fig. 7. Reflection and transmission coefficients as a function of incident angle.

Equation (45) is an infinite-dimensional matrix equation which can be solved numerically by proper truncation.

The solution of (45) is illustrated with applications to electrooptical modulators. We let the three permittivities be equal $\varepsilon_1 = \varepsilon_2 = \varepsilon_3 = \varepsilon$. The various modal amplitudes are plotted as functions of a variable v defined as

$$v = \frac{\pi L}{\lambda}\sqrt{\varepsilon_2}\, M \tag{52}$$

which is directly proportional to the modulation index M. The results are compared with those obtained by Klein and Cook [7] who neglected boundary effects and discarded terms involving second derivatives. The parameter Q in Figs. 5 and 6 is defined to be

$$Q = \frac{2\pi\lambda L}{\sqrt{\varepsilon_2}\, d^2} \tag{53}$$

which is a structure constant determined by the periodicity and the thickness of the slab.

Figs. 5 and 6 show the comparison of our results with the results by Klein and Cook. In Fig. 7 we show a numerical example for reflection and transmission of a plane wave with wavelength $\lambda = 0.6328$ μm by a periodically modulated slab ($\varepsilon_2(z) = 2.32\varepsilon_0[1 + 0.05 \cos(2\pi z/0.665 \times 10^{-6})]$) with periodicity $d = 0.665$ μm and thickness $L = 8$ μm, which corresponds to $v = 3$, $q = 0.256$, and $Q = 47$. The slab is bounded with $\varepsilon = 1$ on one side and $\varepsilon = 3$ on the other side. The sum of the power in all the modes adds to unity.

V. Axis of Modulation Perpendicular to Slab Interfaces

In this case the z axis coincides with the X axis and the x axis is the negative Z axis. We have $\gamma = 90°$.

$$\tilde{\xi}_{v+} = \tilde{\xi}_{v-} = -k_z, \qquad \text{for all } v$$

$$\tilde{\beta}_{n+}^{(v)} = -\tilde{\beta}_{n-}^{(v)} = \tilde{\beta}_n^{(v)} = \tilde{\beta}_0^{(v)} + n\frac{2\pi}{d}$$

$$\left.\begin{aligned} \bar{a}_{n-v}^{(v)} &= a_{n-v}^{(v)} \\ k_{Zn} &= k_Z + n\frac{2\pi}{d}\cos\gamma = k_Z = k\sin\theta_0 \\ k_{Xn} &= k_X = k\cos\theta_0 \\ k_{3Xn} &= k_{3X} = (\varepsilon_3 k_0^2 - k_Z^2)^{1/2}. \end{aligned}\right\}, \qquad \text{for all } n.$$

If we define

$$R = \sum_n R_n \tag{54}$$

$$T = \sum_n T_n \tag{55}$$

then (21) and (22) become

$$E_{1Y}(X,Z) = e^{i(k_X X + k_Z Z)} + Re^{i(-k_X X + k_Z Z)} \tag{56}$$

$$H_{1Z}(X,Z) = \frac{k_X}{\omega\mu_0}\left(e^{i(k_X X + k_Z Z)} - Re^{i(-k_X X + k_Z Z)}\right) \tag{57}$$

and (26) and (27) become

$$E_{3Y}(X,Z) = Te^{ik_{3X}(X-L) + ik_Z Z} \tag{58}$$

$$H_{3Z}(X,Z) = \frac{k_{3X}}{\omega\mu_0} Te^{ik_{3X}(X-L) + ik_Z Z}. \tag{59}$$

In view of (16) and (17), we see that all the v modes are identical, and the modal function becomes

$$\tilde{\phi}_v(z) = \sum_n a_{n-v}^{(v)} e^{i\tilde{\beta}_n^{(v)} z} = \sum_n a_{n-v} e^{i\tilde{\beta}_{n-v}^{(0)} z}. \tag{60}$$

If we let $m = n - v$, (60) becomes

$$\tilde{\phi}_v(z) = \sum_m a_m e^{i\tilde{\beta}_m^{(0)} z} = \tilde{\phi}_0(z), \qquad \text{for all } v. \tag{61}$$

We define

$$\tilde{U} = \sum_v \tilde{U}_v \tag{62}$$

$$\tilde{V} = \sum_v \tilde{V}_v. \tag{63}$$

The fields in region 2 become

$$E_{2Y}(X,Z) = \left[\tilde{U}\sum_n a_n e^{i\tilde{\beta}_n^{(0)}X} + \tilde{V}\sum_n a_n e^{-i\tilde{\beta}_n^{(0)}X}\right] e^{ikzZ} \quad (64)$$

$$H_{2Z}(X,Z) = \left[\tilde{U}\sum_n \frac{\tilde{\beta}_n^{(0)}}{\omega\mu} a_n e^{i\tilde{\beta}_n^{(0)}X} - \tilde{V}\sum_n \frac{\tilde{\beta}_n^{(0)}}{\omega\mu} a_n e^{-i\tilde{\beta}_n^{(0)}X}\right] e^{ikzZ}. \quad (65)$$

The boundary conditions at $X = 0$ and $X = L$ give

$$1 + R = (\tilde{U} + \tilde{V})\sum_n a_n \quad (66)$$

$$k_X(1 - R) = (\tilde{U} - \tilde{V})\sum_n \tilde{\beta}_n^{(0)} a_n \quad (67)$$

$$T = \tilde{U}\sum_n a_n e^{i\tilde{\beta}_n^{(0)}L} + \tilde{V}\sum_n a_n e^{-i\tilde{\beta}_n^{(0)}L} \quad (68)$$

$$k_{3X}T = \tilde{U}\sum_n a_n\tilde{\beta}_n^{(0)} e^{i\tilde{\beta}_n^{(0)}L} - \tilde{V}\sum_n a_n\tilde{\beta}_n^{(0)} e^{-i\tilde{\beta}_n^{(0)}L}. \quad (69)$$

Eliminating R and T from (66)–(69), we obtain

$$\left.\begin{aligned} A\tilde{U} + B\tilde{V} &= 2\\ C\tilde{U} + D\tilde{V} &= 0\end{aligned}\right\} \quad (70)$$

where

$$A = \sum_n (1 + \tilde{\beta}_n^{(0)}/k_X)a_n \quad (71)$$

$$B = \sum_n (1 - \tilde{\beta}_n^{(0)}/k_X)a_n \quad (72)$$

$$C = \sum_n (1 - \tilde{\beta}_n^{(0)}/k_{3X})a_n e^{i\tilde{\beta}_n^{(0)}L} \quad (73)$$

$$D = \sum_n (1 + \tilde{\beta}_n^{(0)}/k_{3X})a_n e^{-i\tilde{\beta}_n^{(0)}L}. \quad (74)$$

Solving (70) for $\tilde{U}$ and $\tilde{V}$, we find

$$\tilde{U} = \frac{2D}{AD - BC} \quad (75)$$

$$\tilde{V} = -\frac{2C}{AD - BC}. \quad (76)$$

We now retain only two modes, $v = 0$ and $v = -1$, in our solutions. Consider the case when the periodicity d and the incident wave number k is in the vicinity of the first Bragg condition for normal incidence $\theta_0 = 0$, then the longitudinal wave number $\tilde{\beta}_0$ takes the following complex values:

$$\tilde{\beta}_0 = (1 + i\alpha)\frac{\pi}{d} \quad (77)$$

and the transverse wave number $\tilde{\xi}_0 = 0$ for normal incidence. For the incident wave satisfying exactly the first Bragg condition, we have $p_0 = \varepsilon_2(k_0 d/\pi)^2 = 1$. When the incident wave is in the vicinity of the first Bragg condition, we define a quantity δ to measure the deviation from the first Bragg condition

$$\delta = \frac{1}{q}[1 - \varepsilon_2(k_0 d/\pi)^2] = \frac{1}{q}(1 - p_0). \quad (78)$$

The dispersion relation for incidence in the vicinity of the first Bragg condition can be approximated as

$$p_0 \approx 1 - \sqrt{q^2 - 4\alpha^2}. \quad (79)$$

Equating (78) and (79) and solving for α, we obtain

$$\alpha = \frac{q}{2}\sqrt{1 - \delta^2}. \quad (80)$$

We shall consider only two dominate space harmonics for each of the two dominate modes, $v = 0$ and $v = -1$, in our solutions. Note that

$$L_{-1}^{0} = (\tilde{\beta}_{-1}d/\pi)^2 - p_0 = \left(-1 + i\frac{q}{2}\sqrt{1 - \delta^2}\right)^2 - (1 - \delta q) = q(\delta - i\sqrt{1 - \delta^2}). \quad (81)$$

We obtain

$$\frac{a_{-1}^{(0)}}{a_0^{(0)}} = -\frac{q}{L_{-1}^{0}} = -(\delta + i\sqrt{1 - \delta^2}). \quad (82)$$

Retaining only two modes in the solution, we then write

$$\tilde{E}_{2Y} = \tilde{U}(a_{-1}e^{i\tilde{\beta}_{-1}^{(0)}z} + a_0 e^{i\tilde{\beta}_0^{(0)}z}) + \tilde{V}(a_{-1}e^{-i\tilde{\beta}_{-1}^{(0)}z} + a_0 e^{-i\tilde{\beta}_0^{(0)}z}) = R(z)e^{i(\pi z/d)} + S(z)e^{-i(\pi z/d)} \quad (83)$$

where

$$R(z) = \tilde{U}a_0 e^{i(\tilde{\beta}_0^{(0)} - (\pi/d))z} + \tilde{V}a_{-1}e^{-i(\tilde{\beta}_0^{(0)} - (\pi/d))z} \quad (84)$$

and

$$S(z) = \tilde{U}a_{-1}e^{i(\tilde{\beta}_0^{(0)} - (\pi/d))z} + \tilde{V}a_0 e^{-i(\tilde{\beta}_0^{(0)} - (\pi/d))z}. \quad (85)$$

In view of (82), we can show that

$$\frac{dR(z)}{dz} + i\left(\frac{q}{2}\frac{\pi}{d}\delta\right)R(z) = -i\left(\frac{q}{2}\frac{\pi}{d}\right)S(z) \quad (86)$$

$$\frac{dS(z)}{dz} - i\left(\frac{q}{2}\frac{\pi}{d}\delta\right)S(z) = i\left(\frac{q}{2}\frac{\pi}{d}\right)R(z). \quad (87)$$

Equations (86) and (87) are the well-known coupled wave equations induced by index coupling as obtained by Kogelnik and Shank [9] in their study of distributed feedback laser systems.

VI. Discussions

The problem of a plane wave incident upon a bounded periodic medium has been solved with the modal approach. The solutions are illustrated for TE waves. In the case of TM wave incidence, the wave equation inside the periodic medium is given by

$$\nabla^2\overline{H}_y + \omega^2\mu\varepsilon(z)\overline{H}_y + \frac{\varepsilon'(z)}{\varepsilon(z)}\frac{\partial}{\partial z}\overline{H}_y = 0$$

instead of (3). Instead of being governed by the Mathieu equation, the TM wave is governed by the general Hill's equation [10]. However, for the case of $M\lambda/d \ll 1$, we can neglect the third term because it varies as $M/\lambda d$ while the first two terms vary as $1/\lambda^2$. We then have an equation identical in form to (3) and the problem can be solved by a parallel treatment.

It is worth pointing out that the modal theory provides the most rigorous approach to the problem of spatially periodic media. Retaining only two modes in the equations, we have derived the popular coupled wave equations from the postulate of small index modulation. The modal theory is shown to reduce to various previously arrived theories under simplified assumptions. Calculations are presented for cases when other theories fail to apply. We stress that the dispersion analysis techniques as discussed in this paper are very useful tools in studying wave behavior pertaining to periodic media. The paper is directed toward applications to optical components in integrated optics systems. Applications of the theory to other fields are topics worthwhile exploring.

References

[1] R. S. Chu and T. Tamir, "Guided-wave theory of light diffraction by acoustic microwaves," *IEEE Trans. Microwave Theory Tech.*, vol. MTT-18, no. 8, pp. 486–504, Aug. 1970.

[2] S. T. Peng, T. Tamir, and H. L. Bertoni, "Theory of periodic dielectric waveguides," *IEEE Trans. Microwave Theory Tech.*, vol. MTT-23, no. 1, pp. 123–133, Jan. 1975.

[3] L. Bernstein and D. Kermisch, "Image storage and reconstruction in volume holography," *Symposium on Modern Optics*, Polytechnic Institute of Brooklyn, pp. 655–680, Mar. 22–24, 1967.

[4] H. Kogelnik, "Coupled wave theory for thick hologram gratings," *Bell Sys. Tech. Journal*, pp. 2909–2947, Nov. 1969.

[5] R. S. Chu and T. Tamir, "Wave propagation and dispersion in space-time periodic media," *Proc. IEE*, vol. 119, no. 7, pp. 797–806, July 1972.

[6] D. A. Pinnow, "Guided lines for the selection of acoustooptic materials," *IEEE J. Quan. Elec.*, vol. QE-6, no. 4, pp. 223–238, Apr. 1970.

[7] W. R. Klein and B. D. Cook, "Unified approach to ultrasonic light diffraction," *IEEE Trans. Sonics and Supersonics*, vol. SU-14, no. 3, pp. 123–134, July 1967.

[8] M. Born and E. Wolf, *Principles of Optics*, Pergamon Press, New York, 1972.

[9] H. Kogelnik and C. V. Shank, "Coupled-wave theory of distributed feedback lasers," *J. Appl. Phys.*, vol. 43, no. 5, pp. 2327–2335, May 1972.

[10] C. Yeh, K. F. Casey, and Z. A. Kaprelian, "Transverse magnetic wave propagation in sinusoidally stratified dielectric media," *IEEE Trans. Microwave Theory Tech.*, vol. MTT-13, pp. 297–302, May 1965.

Generalized Analysis of Parallel Two-Post Mounting Structures in Waveguide

OSMAN L. EL-SAYED

Abstract—**An analytical expression is obtained for the reactance of parallel two-post mounting structures having unsymmetrical strip and gap positions and different strip and gap widths. An equivalent circuit is derived and analytical expressions for its components established giving a physical insight into the problem of coupling between the two gaps. The analysis is based on deriving a variational expression for the structure reactance from the boundary conditions at the structure position. The theoretical results are experimentally verified for a wide range of coupling conditions.**

Exploitation of this model for the design of wide-band varactor-tuned negative resistance oscillators and multidiode parallel mounts in general is discussed.

List of Symbols

$J(r)$	Strip current density.
$I(y)$	Strip current.
I_g	Gap current.
v_g	Voltage drop across gap.
E_{in}	y-directed incident electric field intensity.
$E_r(r)$	y-directed scattered electric field intensity.
$E_g(r)$	Gap field intensity.
R	Reflection coefficient at mount position.
n	Free-space wave impedance equals $\sqrt{u_0/\varepsilon_0}$.
δ_n	Kronecker delta.
m,n	Mode number.
k_x	Equals $m\Pi/a$.
k_y	Equals $n\Pi/b$.
k_{p_m}	Post coupling coefficient equals $\sin k_x S(\sin (k_x W/2)/(k_x W/2))$.
k_{g_n}	Gap coupling coefficient equals $\cos k_y h(\sin (k_y g/2)/(k_y g/2))$.
λ	Free-space wavelength.
λ_g	Guide wavelength (dominant mode).
k	Free-space wave number equals $2\Pi/\lambda$.
Γ_{mn}	Guide wave number equals $\sqrt{k_x^2 + k_y^2 - k^2}$.
k'	Dominant wave number equals $(2\Pi/\lambda_g) = (\Gamma_{10}/j)$.
Z_0	Guide characteristic impedance equals $(2b/a)n(\lambda_g/\lambda)$.
$u(x)$	Distribution function given by

$$u(x) = \begin{cases} 1, & \text{for } S - \dfrac{W}{2} < x < S + \dfrac{W}{2} \\ 0, & \text{elsewhere.} \end{cases}$$

Manuscript received December 23, 1975; revised May 25, 1976.

The author is with the Department of Electronics, University of Provence, Aix-Marseille, France, on leave from the Faculty of Engineering, Cairo University, Cairo, Egypt.